Atmos. Chem. Phys. Discuss., 12, 11079–11103, 2012
www.atmos-chem-phys-discuss.net/12/11079/2012/
doi:10.5194/acpd-12-11079-2012
© Author(s) 2012. CC Attribution 3.0 License.

Atmospheric Chemistry and Physics Discussions

This discussion paper is/has been under review for the journal Atmospheric Chemistry and Physics (ACP). Please refer to the corresponding final paper in ACP if available.

Emissions of mercury in Southern Africa derived from long-term observations at Cape Point, South Africa

E.-G. Brunke[1], **R. Ebinghaus**[2], **H. H. Kock**[2], **C. Labuschagne**[1], **and F. Slemr**[3]

[1]South African Weather Service c/o CSIR, P.O. Box 320, Stellenbosch 7599, South Africa
[2]Helmholtz-Zentrum Geesthacht, Institute of Coastal Research, Max-Planck-Strasse, 21502 Geesthacht, Germany
[3]Max-Planck-Institut für Chemie, P.O. Box 3060, 55020 Mainz, Germany

Received: 19 February 2012 – Accepted: 19 April 2012 – Published: 2 May 2012

Correspondence to: F. Slemr (franz.slemr@mpic.de)

Published by Copernicus Publications on behalf of the European Geosciences Union.

Abstract

Mercury emissions in South Africa have so far been estimated only by a bottom-up approach from activities and emission factors for different processes. In this paper we derive GEM/CO (GEM being gaseous elemental mercury, Hg^0), GEM/CO_2, GEM/CH_4, CO/CO_2, CH_4/CO_2, and CH_4/CO emission ratios from plumes observed during long-term monitoring of these species at Cape Point between March 2007 and December 2009. The average observed GEM/CO, GEM/CO_2, GEM/CH_4, CO/CO_2, CH_4/CO_2, and CH_4/CO emission ratios were $2.40 \pm 2.65\,pg\,m^{-3}\,ppb^{-1}$ ($n = 47$), $62.7 \pm 80.2\,pg\,m^{-3}\,ppb^{-1}$ ($n = 44$), $3.61 \pm 4.66\,pg\,m^{-3}\,ppb^{-1}$ ($n = 46$), $35.6 \pm 25.4\,ppb\,ppm^{-1}$ ($n = 52$), $20.2 \pm 15.5\,ppb\,ppm^{-1}$ ($n = 48$), and $0.876 \pm 1.106\,ppb\,ppb^{-1}$ ($n = 42$), respectively. The observed CO/CO_2, CH_4/CO_2, and CH_4/CO emission ratios agree within the combined uncertainties of the observations and emissions with the ratios calculated from EDGAR (version 4.2) CO_2, CO, and CH_4 inventories for South Africa and Southern Africa (South Africa, Lesotho, Swaziland, Namibia, Botswana, Zimbabwe, and Mozambique) in 2007 and 2008 (inventories for 2009 are not available yet). Total elemental mercury emission of 13.1, 15.2, and 16.1 $t\,Hg\,yr^{-1}$ are estimated independently using the GEM/CO, GEM/CO_2, and GEM/CH_4 emission ratios and the annual mean CO, CO_2, and CH_4 emissions, respectively, of South Africa in 2007 and 2008. The average of these independent estimates of $14.8 \pm 1.5\,t\,GEM\,yr^{-1}$ is much less than the total emission of $257\,t\,Hg\,yr^{-1}$ from older inventories. Considering that emission of GEM represents only 50–78 % of all mercury emissions, our estimates come close to the total mercury emission estimates ranging between 40–50 $t\,Hg\,yr^{-1}$ from more recent inventories.

1 Introduction

Mercury emissions to the atmosphere are of global importance because of its long range transport, deposition and partial transformation to highly neurotoxic methyl

ACPD
12, 11079–11103, 2012

mercury. The latter is then bio-accumulated in the aquatic nutrition chain and may affect both human populations and fauna which are dependent on fish (Mergler et al., 2007; Scheuhammer et al., 2007). Emissions from different natural and anthropogenic processes such as volcanic emissions, emissions from soil and coal as well as biomass burning have thus been determined and the spatially and temporally resolved emission inventories calculated from the emission factors obtained in these studies (e.g., Nriagu and Pacyna, 1988; Nriagu, 1989; Pirrone et al., 1996, 1998, 2010; Pacyna et al., 2002, 2003, 2006, 2010; Streets et al., 2005, 2009). Despite all these efforts the emission estimates are still quite uncertain, especially those related to natural sources and anthropogenic emissions in rapidly developing countries in East and South-East Asia (Lin et al., 2006; Lindberg et al., 2007; Pacyna et al., 2010; Pirrone et al., 2010).

Emissions from Southern Africa are one example of these uncertainties. In emission inventories for 1995 and 2000 South Africa and especially its provinces Gauteng and Mpumalanga were supposed to represent the region with the highest mercury emission density within the Southern Hemisphere (Pacyna et al., 2003; Wilson et al., 2006). The emissions were attributed to coal burning and gold production in equal parts. Whereas the emissions from coal burning are reasonably well documented, the large emission from gold production has been found to be incorrect as industrial gold production in South Africa relies almost exclusively on cyanide technology which does not emit mercury (Dabrowski et al., 2008; Leaner et al., 2009; Masekoameng et al., 2011). According to the more recent inventories the mercury emissions in South Africa amounted to 40 t Hg yr^{-1} in 2004 (Leaner et al., 2009) and 50 t Hg yr^{-1} in 2006 (Masekoameng et al., 2010).

All emission estimates mentioned above represent a bottom-up approach in which emissions from different individual processes are estimated from the activities, their corresponding emission factors and the resulting emissions are then summed up. On a global scale, 3-D-models in combination with observations were used to constrain the emission estimates (e.g., Selin et al., 2007, 2008; Strode et al., 2007). However, the uncertainty of these constraints is seldom smaller than that of the emission inventories.

ACPD
12, 11079–11103, 2012

In addition, such global constraints do not provide much information about regional emission densities. At regional and local scales the emission inventories can be constrained directly by observations (e.g., Jaffe et al., 2005; Slemr et al., 2002, 2006). In this paper we analyze the pollution events observed at Cape Point during the period between March 2007 and December 2009. GEM/CO, GEM/CO_2, GEM/CH_4, CO/CO_2, CH_4/CO_2, and CH_4/CO emission ratios are calculated from the correlations of these species during pollution events and GEM emissions are then calculated from known CO, CO_2, and CH_4 emissions in South Africa. In addition the GEM/CO, GEM/CO_2, and GEM/CH_4 emission ratios for plumes which according to the backward trajectories originate from the Gauteng and Mpumalanga provinces are compared with emission ratios from other regions.

2 Experimental

The Cape Point station (34° 21′ S, 18° 29′ E) is part of the World Meteorological Organization's (WMO) Global Atmosphere Watch (GAW) network. Cape Point is about 60 km south of Cape Town, and located on top of a coastal cliff 230 m a.s.l. at the southernmost tip of the Cape Peninsula. The site is located in a nature reserve and experiences moderate temperatures, dry summers with occasional biomass burning episodes in the surrounding area and increased precipitation during austral winter. The dominant wind direction is from the south-eastern sector which is representative of clean maritime air from the Southern Ocean (Brunke et al., 2004). The site is occasionally also subjected to air from the northern to north-eastern sector (mainly during austral winter), which is influenced by anthropogenic emissions from the greater Cape Town area and/or by other continental sources.

Within the framework of the WMO-GAW program, continuous trace gas measurements of CO_2, CH_4, CO and O_3 have been made at Cape Point for more than 25 yr (Scheel et al., 1990). Gaseous mercury concentrations have been measured discontinuously (about 200 samples per year) since September 1995 (Baker et al.,

ACPD
12, 11079–11103, 2012

2002) and continuously with a resolution of 15 min since March 2007 (Brunke et al., 2010).

Continuous measurements of gaseous mercury are made using a Tekran 2537A vapor-phase mercury analyzer manufactured by Tekran Inc., Toronto, Canada. It is capable of measuring low level mercury concentrations typically observed at background locations (Ebinghaus et al., 1999; Munthe et al., 2001). The analyzer is operated in an air-conditioned laboratory and run with a sampling air flow rate of 1 l min^{-1} at 15 min sampling intervals. The mercury detection limit under these conditions is about 0.05 ng m^{-3} and the span of the analyzer is checked by an internal permeation source once every 25 h. The air sample intake was attached to a 30-m high aluminum sampling mast at a height of approximately 5 m above the rocky surface and about 235 m a.s.l. A Teflon filter (pore size 0.2 µm; ID = 45 mm) upstream of the instrument protects the analyzer against contamination by particulate matter. The filter has been replaced once every two weeks. The 15-min mercury data have been converted to 30-min averages so that comparisons with other trace gas and meteorological data being measured simultaneously at Cape Point could be made. Under the prevailing atmospheric conditions at Cape Point (higher temperature and air humidity, in addition to hygroscopic sea salt aerosols) we assume that reactive gaseous mercury (RGM) will be adsorbed by the inlet tubing and the aerosol filter and that the measured atmospheric mercury concentration thus represents exclusively gaseous elemental mercury (GEM) (Brunke et al., 2010). All mercury data concentrations are given as ng m^{-3} (STP) with a standard temperature of 273.16 K and pressure of 1013 mbar.

Carbon monoxide has been measured at Cape Point since December 1989 with a model RGA-3 (Trace Analytical, Stanford, California) instrument. The analytical principle is the reduction of HgO by CO to Hg vapor and its subsequent detection by atomic absorption at 254 nm. CH_4 measurements started in 1982 and are made by the well established GC-FID technique making use of a 13X molecular sieve column. Carbon dioxide has been measured since 1992 with a URAS 4T NDIR analyzer. The measurements of all three trace gases are linked to the NOAA-ESRL scale.

ACPD
12, 11079–11103, 2012

The uncertainties (expressed as percentage variations at currently observed background levels) for CO_2, CH_4, and CO amount to 0.01, 0.2, and 4.0, respectively. Analytical details of the atmospheric parameters measured have been summarized under www.empa.ch/gaw/gawsis and have also been described in previous publications (Brunke et al., 1990; Scheel et al., 1990; WMO, 2005).

Jaffe et al. (2005) uses the slopes of the X vs. Y correlations as emission ratios under assumptions of (a) no losses of the substances during the transport, (b) constant source with fixed emission ratios, and (c) constant background concentration during the event. The assumption (b) can be extended for multiple sources along the trajectory of an event if their relative contribution remains constant during the event. As the events last on average 7.2 h and none lasts more than 17.5 h, these assumptions are reasonable. GEM vs. CO, CO_2, CH_4, CO and CH_4 vs. CO_2, and CH_4 vs. CO were all correlated using orthonormal regression (Cantrell, 2008) which takes the uncertainties of the measurements of both correlated parameters into account. These uncertainties were set to 0.05 ng m^{-3}, 1 ppb, 0.05 ppm, and 2 ppb for mercury, CO, CO_2, and CH_4, respectively. The individual correlations are listed in the supporting materials. Four significant correlations with negative slopes were not considered in the statistical analysis.

The regions of origin for the pollution events were interpreted using ten-day isentropic backward trajectories from NOAA ESRL (http://www.esrl.noaa.gov/gmd) and seven-day back trajectories calculated by NILU using FLEXTRA model (http://nadir.nilu.no/trajectories/modeldata/2012 and http://nadir.nilu.no/trajectories/files/png/2012). The GEM emissions were calculated using the CO, CO_2, and CH_4 emission data for 2007 and 2008 from Emission Database for Global Atmospheric Research (EDGAR), version 4.2. The data for 2009 are not available yet.

ACPD
12, 11079–11103, 2012

3 Results and discussion

3.1 Statistics of pollution events

Pollution events (PEs) were defined as events with GEM concentrations of 0.18 ng m^{-3} above the eleven day moving average (Brunke et al., 2010). Altogether 67 events were identified for the period starting in March 2007 and ending in December 2009. Their seasonal frequency in Fig. 1 shows that most of them occur only during one half of the year, i.e. from March until August. Only two PEs per month were observed during January, February and September and none in October, November and December. This is in agreement with the climatology of the site where the predominant wind direction is from the ocean during austral summer with a higher incidence of air flow from the northern and north-eastern sectors during austral winter (Brunke et al., 2010).

Table 1 provides an overview of the data availability, the number of significant positive correlations (at a significance level of > 95 %) of GEM with CO, CO_2, CH_4, of CO with CO_2, and of CH_4 with CO_2 and CO, the range, average, and median of the corresponding regression slopes. CO and CH_4 correlated with CO_2 most frequently (83 and 76 % of all PEs with available data, respectively), followed by GEM vs. CO, CO_2, and CH_4 (70, 70, and 69 %, respectively). CH_4 vs CO correlated least frequently with 63 % of all PEs with available data. The calculated slopes span a range which is generally two orders of magnitude, and the slope medians are usually only about half as large as the slope average. This suggests a strongly skewed distribution of the slopes for all correlations.

3.2 Observed emission ratios

The correlation slopes for GEM vs. CO range from 0.20 to 11.5 pg m^{-3} ppb^{-1}, while their average and median values amounted to 2.40±2.65 (n = 47) and 1.41 pg m^{-3} ppb^{-1}, respectively. The standard error of the average GEM/CO emission ratio, considered by us as relevant for the analysis of uncertainty of emission estimates, is 0.39 pg m^{-3} ppb^{-1},

ACPD
12, 11079–11103, 2012

i.e. 16 % of the average. Figure 2 shows that 27 slopes are located within the 0.5–2.0 $pg\,m^{-3}\,ppb^{-1}$ range, while three slopes fall below it. Fourteen slopes range from 2 to 12 $pg\,m^{-3}\,ppb^{-1}$. The median slope of 1.41 $pg\,m^{-3}\,ppb^{-1}$ and even the average slope are much smaller than the average slope of 5.0 ± 2.1 $pg\,m^{-3}\,ppb^{-1}$ observed between 1996 and 2003 at Mace Head in plumes originating from Europe (Slemr et al., 2006) and 5.6 ± 1.6 $pg\,m^{-3}\,ppb^{-1}$ observed in 2004 at Hedo Station, Okinawa, in plumes originating from East Asia (Jaffe et al., 2005). However, the predominant range of 0.5–2.0 $pg\,m^{-3}\,ppb^{-1}$ falls within the range of 0.7–2.2 $pg\,m^{-3}\,ppb^{-1}$ of emission ratios observed in the plumes from biomass burning (Friedli et al., 2009). This suggests that most of the plumes originated from biomass burning or were substantially influenced by it. This is not surprising. Biomass burning in Southern Africa (according to EDGAR inventory mostly savanna burning, burning of agricultural waste, forest and grassland fires) starts usually in May, peaks in July–September and ceases in November (Duncan et al., 2003; van der Werf et al., 2006). This seasonal variation overlaps with the seasonal frequency of our plume observations shown in Fig. 1 with most plumes occurring between March and August.

The GEM/CH_4 slopes range from 0.37 to 24.8 $pg\,m^{-3}\,ppb^{-1}$ with an average of 3.61 ± 4.66 $pg\,m^{-3}\,ppb^{-1}$ ($n = 46$) and a median of 2.13 $pg\,m^{-3}\,ppb^{-1}$. The standard error of the average GEM/CH_4 emission ratio is 0.69 $pg\,m^{-3}\,ppb^{-1}$, i.e. 19 % of the average. The distribution of the GEM/CH_4 emission ratios is shown in Fig. 2. The emission ratio observed at Mace Head in European plumes varied between 2.2 and 5.6 $pg\,m^{-3}\,ppb^{-1}$. Methane is emitted from many sources among which the biomass burning, leakage during coal and natural gas extraction, enteric fermentation and agricultural rice cultivation are the more important ones (Clerbaux and Cunnold, 2007; EDGAR inventory). Since none of these sources is dominant (Clerbaux and Cunnold, 2007; EDGAR inventory), the Hg/CH_4 emission cannot be used to attribute the origin of these emissions.

The GEM/CO_2 slopes range from 12.3 to 436 $pg\,m^{-3}\,ppm^{-1}$ with an average of 62.7 ± 80.2 $pg\,m^{-3}\,ppm^{-1}$ ($n = 44$) and a median of 34.1 $pg\,m^{-3}\,ppm^{-1}$. The standard

ACPD
12, 11079–11103, 2012

error of the average GEM/CO_2 emission ratio is 12.1 pg m^{-3} ppm^{-1}, i.e. 19 % of the average. Figure 2 shows a frequency distribution of the Hg/CO_2 slopes with 26 slopes falling within the range of 10–40 pg m^{-3} ppm^{-1} and 9 slopes in the range between 40–80 pg m^{-3} ppm^{-1}. Eight slopes are larger than 110 pg m^{-3} ppm^{-1}. There is a lack of information on GEM/CO_2 emission ratios from different types of burning. To the best of our knowledge the only emission ratio for biomass burning (109 ± 27 pg m^{-3} ppm^{-1}) has so far been reported by Brunke et al. (2001) for a biomass fire close to Cape Point. Taking the average Hg content of coal (0.29 g Hg Mg^{-1} coal) into account as well as the average Hg emission reduction of 0.39 due to flue cleaning in South African power plants (Leaner et al., 2009), an average emission ratio of about 15 pg m^{-3} ppm^{-1} can be estimated for the power plant plumes. Since the coal Hg content varies from 0.15 to 0.45 µg Hg g^{-1} coal and the flue cleaning process can remove 50–90 % of mercury, the emission ratio can be expected to vary from about 2 to 30 pg m^{-3} ppm^{-1}.

The correlation slopes of CO vs. CO_2 range from 3.98–169 ppb ppm^{-1}, while their average and median values amount to 35.6 ± 25.4 (n = 52) and 30.1 ppb ppm^{-1}, respectively. The standard error of the average CO/CO_2 emission ratio is 3.52 ppb ppm^{-1}, i.e. 10 % of the average. Figure 2 shows that except for one event with slope exceeding 100 ppb ppm^{-1} all other slopes are smaller than 70 ppb ppm^{-1}. The emission ratios for biomass burning vary from about 60 ppb ppm^{-1} for grassland savannas up to about110 ppb ppm^{-1} for extra tropical forests (Andreae and Merlet, 2001; Singh et al., 2010), while the emission ratios for fossil fuel burning varies between 5 and 25 ppb ppm^{-1} (Gamnitzer et al., 2006; Singh et al., 2010). Thirteen of the slopes are smaller than 20 ppb ppm^{-1} suggesting that fossil fuel burning contributes substantially to the plumes observed at Cape Point.

The CH_4/CO_2 slopes range from 1.05 to 77.3 ppb ppm^{-1} with an average of 20.2 ± 15.5 ppb ppm^{-1} (n = 48) and a median of 15.7 ppb ppm^{-1}. The standard error of the average is 2.24 ppb ppm^{-1}, i.e. 11 % of the average. Their frequency distribution in Fig. 2 is skewed with most of the slopes being in the range of 1.1–40 ppb ppm^{-1}. The CH_4/CO_2 emission ratio of biomass burning varies between 3.9 and 11.8 ppb ppm^{-1}

ACPD
12, 11079–11103, 2012

(Andreae and Merlet, 2001). The distribution of the CH_4/CO_2 slopes and their average and median thus again suggest that biomass burning is just one of several CH_4 sources.

The CH_4/CO slopes range from 0.092 to 6.62 ppb ppb^{-1} with an average of 0.877 ± 1.106 ppb ppb^{-1} (n = 42) and a median of 0.509 ppb ppb^{-1}. The standard error of the average is 0.171 ppb ppb^{-1}, i.e. 20 % of the average. The frequency distribution in Fig. 2 shows a skewed distribution with a pronounced peak at 0.25–0.5 ppb ppb^{-1}, and nine slopes above 1.0 ppb ppb^{-1}. For plumes observed over North America Singh et al. (2010) reported ratios of 0.08 ± 0.03 ppb ppb^{-1} for plumes of fresh biomass burning, 0.25±0.10 ppb ppb^{-1} for a mixture of urban and aged biomass burning plumes, and 1.1 ± 1.1 ppb ppb^{-1} for urban plumes, making the CH_4/CO emission ratio a good indicator for the origin of the plumes. Apart from 4 slopes above 2 ppb ppb^{-1} the observations fall into all three categories.

3.3 Geographical origin of the PEs

According to the geographical distribution by Wilson et al. (2006) most of the mercury emissions in Southern Africa are located in the eastern part of South Africa – more particularly in the provinces of Gauteng and Mpumalanga in the northeast. Since mercury emissions from gold production are assumed to be responsible for about half of all emissions in the older inventories and gold production is an unlikely source of CO and CH_4, the GEM/CO and GEM/CH_4 emission ratios for events originating from this region should differ from those of other regions. To investigate this we classified the pollution events according to their backward trajectories into 4 groups: (1) North-West Cape (with a subgroup 1 (CT): Cape Town), (2) Gauteng, Mpumalanga, Botswana, Zimbabwe, (3) East Cape Province, (4) marine with short section over the continent. Figure 3 displays an example of a typical backward trajectory for each group. Most of the pollution events were embedded in marine air with only a short section over the continent (group 4, 25 events), followed by pollution events originating from Namibia,

ACPD
12, 11079–11103, 2012

the Northern West Cape Province and Cape Town (group 1, 11 events). Only a few pollution events originated in Gauteng, Mpumalanga, Botswana, and Zimbabwe (group 2, 8 events) and East Cape Province (group 3, 5 events). The low frequency of pollution events with origin over the industrialized Highveld region is in agreement with the general transport pattern described by Freiman and Piketh (2003).

Table 2 shows the averages and medians of GEM/CO, GEM/CO_2, GEM/CH_4, CO/CO_2, CH_4/CO_2, and CH_4/CO emission ratios for the different trajectory groups. The average emission ratios for different trajectory groups differ by about a factor of 3 for GEM/CO, GEM/CO_2, and GEM/CH_4 and less than a factor of 2 for CO/CO_2, CH_4/CO_2, and CH_4/CO suggesting that the distribution of GEM emissions might be more inhomogeneously distributed than those of CO, CO_2, and CH_4. Unfortunately, none of the differences is statistically significant due to the large standard deviations and a small number of events falling in categories 2 and 3. Thus we conclude that there is no sign of extraordinary high GEM/CO, GEM/CO_2, and GEM/CH_4 emission ratios in pollution plumes originating in the provinces of Mpumalanga and Gauteng. This finding is consistent with the emission estimates by Dabrowski et al. (2008), Leaner et al. (2009), and Masekoameng et al. (2011) who deem substantial mercury emissions from gold production non-existent because of the use of cyanide extraction process.

3.4 GEM emission estimates

Before proceeding to the estimation of the GEM emissions we compare in Table 3 the observed CO/CO_2, CH_4/CO_2, and CH_4/CO emission ratios with those calculated from CO, CO_2, and CH_4 emissions in EDGAR inventory. As many trajectories also cross the territory of the neighbor countries (category 1, 2, and 3) we additionally make calculations with the sum of emissions of South Africa, Swaziland, Lesotho, Namibia, Botswana, Zimbabwe, and Mozambique, termed here as Southern Africa. The CO_2, CO, and CH_4 emissions in Table 3 are average emissions for the years 2007 and 2008, the data for 2009 are not available yet. Table 3 shows that the emissions of South Africa are dominant, representing 83, 70, and 70 % of CO_2, CO, and CH_4

ACPD
12, 11079–11103, 2012

emissions of Southern Africa, respectively. The observed average CO/CO_2 emission ratio of 35.6 ± 25.4 ppb ppm^{-1} ($n = 52$) is significantly higher than the calculated ratios of 23.0 and 27.2 ppb ppm^{-1} for South Africa and Southern Africa, respectively. The difference is with 55 % larger for South Africa than 31 % for Southern Africa. The median CO/CO_2 emission ratio of 30.1 ppb ppm^{-1} is closer to the calculated one for Southern Africa but still 31 % above the calculated one for South Africa. The differences between observed average CH_4/CO_2 and CH_4/CO emissions and those calculated for South Africa and Southern Africa are not significant and except for CH_4/CO_2 they lie between the median and the average emission ratios. This comparison does take neither the uncertainties of emission inventories into accounts nor the uncertainties of the observed emission ratios. The emission uncertainties are estimated to be about 10 % for CO_2 and 50 % for each CO and CH_4 (Olivier et al., 2001). The uncertainties of the observed emission ratios are represented by the standard errors of the averages, i.e. of 10 %, 11 %, and 20 % for CO/CO_2, CH_4/CO_2, and CH_4/CO, respectively. A small additional uncertainty originates from using the average annual emissions for 2007 and 2008 while the observations cover 2009 as well for which the emissions are not available yet. Taking all these uncertainties into account we conclude that the CO/CO_2, CH_4/CO_2 and CH_4/CO emission ratios observed at Cape Point reproduce reasonably well the emission ratios for South Africa and Southern Africa calculated from the EDGAR inventory. This agreement lends credence to the GEM emission estimates below.

GEM emission of 13.1, 15.2 and 16.1 t Hg yr^{-1} are estimated from GEM/CO, GEM/CO_2, and GEM/CH_4 emission ratios, respectively, and the South African emissions of CO, CO_2, and CH_4. The average of these three independent estimations is 14.8 ± 1.5 t Hg yr^{-1}. Using the CO, CO_2, and CH_4 emissions of Southern Africa and the corresponding emission ratios, the GEM emissions would be 18.3, 18.6, and 22.9 t Hg yr^{-1}, with an average of 19.9 ± 2.6 t Hg yr^{-1}. The variation coefficients of 10 and 13 % of the three independent GEM emission estimates for South Africa and Southern Africa, respectively, are much smaller than the combined uncertainties discussed above. This demonstrates the consistency of our GEM emission estimates. We would

ACPD
12, 11079–11103, 2012

like to emphasize that all above estimates are for elemental mercury only, the species measured by the instrument at Cape Point. Oxidized mercury (Hg^{2+}) and mercury bound to particles (Hg_P) are not included, because Hg^{2+} gets lost in the inlet tubing of the instrument and particles are filtered out.

Total elementary mercury emission of $14.8\,t\,yr^{-1}$ in South Africa is more than one order of magnitude lower than $256.7\,t\,Hg\,yr^{-1}$ estimated by Pacyna et al. (2003, 2006) but they come close to estimates of $40\,t\,Hg\,yr^{-1}$ in 2004 by Leaner et al. (2009) and $50\,t\,Hg\,yr^{-1}$ in 2006 by Masekoameng et al. (2010) which also include emissions of oxidized and particle bound mercury. GEM represents 53 % of total worldwide emissions (Pacyna et al., 2006), and 50–78 % of emissions of coal powered stations (Pacyna and Pacyna, 2002; Streets et al., 2005), depending on the flue cleaning technology. Assuming GEM to constitute 53 % of all mercury emissions in South Africa, the GEM emissions derived from the emission inventories by Leaner et al. (2009) and Masekoameng et al. (2010) would be 21.2 and $26.5\,t\,Hg\,yr^{-1}$, respectively. This is somewhat higher than the average of our estimates but still within the range of uncertainties discussed above.

Taking all these uncertainties into account, the observed GEM emission is in reasonable agreement with the current mercury inventories for South Africa. The observations and the current inventories thus clearly document that a hot spot for mercury emissions in South Africa postulated by earlier inventories does not exist.

4 Conclusions

Sixty seven pollution events have been identified over the period from March 2007 until December 2009 and analysed for the following emission ratios: GEM/CO, GEM/CO_2, GEM/CH_4, CO/CO_2, CH_4/CO_2, and CH_4/CO. Most of the events occurred between March and August which overlaps with the seasonal occurrence of biomass burning in Southern Africa starting in May, peaking in July–September, and ending in November.

ACPD
12, 11079–11103, 2012

GEM correlation with CO, CO_2, and CH_4, was significant (> 95 %) in 47, 44, and 46 events, respectively. Correlations of CO vs. CO_2, CH_4 vs. CO_2, and CH_4 vs. CO were significant in 52, 48 and 42 events, respectively. Half of the GEM vs. CO slopes fell within the 0.5–2.0 $pg\,m^{-3}\,ppb^{-1}$ range, which matches the range observed by others for biomass burning plumes. Similarly, 30 % of the CO/CO_2 emission ratios fall within the range between 4 and 25 $ppb\,ppm^{-1}$ which also suggests that fossil fuel burning constitutes a substantial fraction of the plumes reaching Cape Point. CH_4/CO emission ratios span a range from 0.09 to 6.6 $ppb\,ppb^{-1}$, indicating contributions of fresh biomass burning, a mixture of aged biomass burning and urban plumes, as well as urban plumes per se. Although information on GEM/CO_2 and GEM/CH_4 ratios in the literature is lacking, their emission ratios of 12–436 $pg\,m^{-3}\,ppm^{-1}$ and 0.37–24.8 $pg\,m^{-3}\,ppb^{-1}$, respectively, confirm the above conclusions that the origin of the observed plumes includes fresh and aged biomass burning as well as plumes from urban areas.

The pollution events were subdivided into 4 groups according to their origin as indicated by backward trajectories. Only 8 events can be ascribed as having originated in the provinces of Gauteng and Mpumalanga where gold production as well as a majority of coal-fired power stations are located. However, no exceptionally high GEM/CO, GEM/CO_2, and GEM/CH_4 emission ratios were found for these events. This supports the contention of Dabrowski et al. (2008), Leaner et al. (2009), and Masekoameng et al. (2011) that gold production does not contribute substantially to mercury emissions in South Africa. However, it should be noted that from an ecosystem perspective this does not necessarily imply that cyanide-leaching is the preferable or more sustainable way for gold production.

The total emission of elemental mercury of $14.8 \pm 1.5\,t\,GEM\,yr^{-1}$ derived from GEM/CH_4, GEM/CO_2, and GEM/CO emission ratios is in reasonable agreement with the current mercury inventories by Dabrowski et al. (2008), Leaner et al. (2009), and Masekoameng et al. (2011) when speciation, the uncertainty of the inventories, and the uncertainty of the observed emission ratios are taken into account. We thus conclude

ACPD
12, 11079–11103, 2012

that the hot spot of mercury emissions postulated by older emission inventories for Southern Africa does not exist.

Supplementary material related to this article is available online at: http://www.atmos-chem-phys-discuss.net/12/11079/2012/acpd-12-11079-2012-supplement.zip.

Acknowledgements. We are grateful towards D. van der Spuy for having assisted in data preparation. By the same token the assistance rendered by B. Parker and T. Mkololo in maintaining the Tekran 2537A analyzer at Cape Point in good working order has been greatly appreciated. We thank J. Williams from KNMI for the EDGAR emission data and the information about their uncertainty. Furthermore, we are also grateful towards NOAA and NILU for having made available backward trajectories.

References

Andreae, M. O. and Merlet, P.: Emissions of trace gases and aerosols from biomass burning, Global Biogeochem. Cy., 15, 955–966, 2001.

Baker, P. G. L., Brunke, E.-G., Slemr, F., and Crouch, A. M.: Atmospheric mercury measurements at Cape Point, South Africa, Atmos. Environ., 36, 2459–2465, 2002.

Brunke, E.-G., Scheel, H. E., and Seiler, W.: Trends of tropospheric CO, N_2O and CH_4 as observed at Cape Point, South Africa, Atmos. Environ., 24, 585–595, 1990.

Brunke, E.-G., Labuschagne, C., and Slemr, F.: Gaseous mercury emissions from a fire in the Cape Peninsula, South Africa, during January 2000, Geophys. Res. Lett., 28, 1483–1486, 2001.

Brunke, E.-G., Labuschagne, C., Parker, B., Scheel, H. E., Whittlestone, S.: Baseline air mass selection at Cape Point, South Africa: application of ^{222}Rn and other filter criteria to CO_2, Atmos. Environ., 38, 5693–5702, 2004.

Brunke, E.-G., Labuschagne, C., Ebinghaus, R., Kock, H. H., and Slemr, F.: Gaseous elemental mercury depletion events observed at Cape Point during 2007–2008, Atmos. Chem. Phys., 10, 1121–1131, doi:10.5194/acp-10-1121-2010, 2010.

ACPD

12, 11079–11103, 2012

Cantrell, C. A.: Technical Note: Review of methods for linear least-squares fitting of data and application to atmospheric chemistry problems, Atmos. Chem. Phys., 8, 5477–5487, doi:10.5194/acp-8-5477-2008, 2008.

Clerbaux, C. and Cunnold, D. M.: Long-lived compounds, in: Scientific Assessment of Ozone Depletion: 2006, WMO, Report No. 50, Geneva, Switzerland, 2007.

Dabrowski, J. M., Ashton, P. J., Murray, K., Leaner, J. J., and Mason, R. P.: Anthropogenic mercury emissions in South Africa: coal combustion in power plants, Atmos. Environ., 42, 6620–6626, 2008.

Duncan, B. N., Martin, R. V., Staudt, A. C., Yevich, R., and Logan, J. A.: Interannual and seasonal variability of biomass burning emissions constrained by satellite observations, J. Geophys. Res., 108, 4100, doi:10.1029/2002JD002378, 2003.

Ebinghaus, R., Jennings, S. G., Schroeder, W. H., Berg, T., Donaghy, T., Guentzel, J., Kenny, C., Kock, H. H., Kvietkus, K., Landing, W., Mühleck, T., Munthe, J., Prestbo, E. M., Schneeberger, D., Slemr, F., Sommar, J., Urba, A., Wallschläger, D., and Xiao, Z.: International field intercomparison measurements of atmospheric mercury species at Mace Head, Ireland, Atmos. Environ., 33, 3063–3073, 1999.

Freiman, M. T. and Piketh, S. J.: Air transport into and out of the industrial Highveld region of South Africa, J. Appl. Meteorol., 42, 994–1002, 2003.

Friedli, H. R., Arellano, A. F., Cinnirella, S., and Pirrone, N.: Mercury emissions from global biomass burning: spatial and temporal distribution, in: Mercury Fate and Transport in the Global Atmosphere, edited by: Pirrone, N. and Mason, R., Springer, Dordrecht, 193–220, 2009.

Gamnitzer, U., Karstens, U., Kromer, B., Neubert, R. E. M., Meijer, H. A. J., Schroeder, H., and Levin I.: Carbon monoxide: a quantitative tracer for fossil fuel CO_2?, J. Geophys. Res., 111, D22302, doi:10.1029/2005JD006966, 2006.

Jaffe, D., Prestbo, E., Swartzendruber, P., Weiß-Penzias, P., Kato, S., Takami, A., Hatakeyama, S., and Kajii, Y.: Export of atmospheric mercury from Asia, Atmos. Environ., 39, 3029–3028, 2005.

Leaner, J. J., Dabrowski, J. M., Mason, R. P., Resane, T., Richardson, M., Ginster, M., Gericke, G., Petersen, C. R., Masekoameng, E., Ashton, P. J., and Murray, K.: Mercury emissions from point sources in South Africa, in: Mercury Fate and Transport in the Global Atmosphere, edited by: Pirrone, N. and Mason, R., Springer, Dordrecht, 113–130, 2009.

ACPD
12, 11079–11103, 2012

Lin, C.-J., Pongprueksa, P., Lindberg, S. E., Pehkonen, S. O., Byun, D., and Jang, C.: Scientific uncertainties in atmospheric mercury models. I: model science evaluation, Atmos. Environ., 40, 2911–2928, 2006.
Lindberg, S., Bullock, R., Ebinghaus, R., Engstrom, D., Feng, X., Fitzgerald, W., Pirrone, N., Prestbo, E., and Seigneur, C.: A synthesis of progress and uncertainties in attributing the sources of mercury in deposition, Ambio, 36, 19–32, 2007.
Masekoameng, K. E., Leaner, J., and Dabrowski, J.: Trends in anthropogenic mercury emissions estimated for South Africa during 2000–2006, Atmos. Environ., in press, 2012.
Mergler, D., Anderson, H. A., Chan, L. H. M., Mahaffey, K. R., Murray, M., Sakamoto, M., and Stern, A. H.: Methyl mercury exposure and health effects in humans: a worldwide concern, Ambio, 36, 3–11, 2007.
Munthe, J., Wängberg, I., Pirrone, N., Iverfeldt, A., Ferrara, R., Ebinghaus, R., Feng, X., Gardfeldt, K., Keeler, G., Lanzillotta, E., Lindberg, S. E., Lu, J., Mamane, Y., Prestbo, E., Schmolke, S., Schroeder, W. H., Sommar, J., Sprovieri, F., Stevens, R. K., Stratton, W., Tuncel, G., and Urba, A.: Intercomparison of methods for sampling and analysis of atmospheric mercury species, Atmos. Environ., 35, 3007–3017, 2001.
Nriagu, J. O.: A global assessment of natural sources of atmospheric trace metals, Nature, 338, 47–49, 1989.
Nriagu, J. O. and Pacyna, J. M.: Quantitative assessment of worldwide contamination of air, water and soils by trace metals, Nature, 333, 134–139, 1988.
Olivier, J. G. J., Berdowski, J. J. M., Peters, J. A. H. W., Bakker, J., Visschedijk, A. J. H., and Bloos, J.-P. J.: Application of EDGAR 3.0: refernce data base with trand data for 1970–1995, report no. 773301, 001/NOP report no. 410200051, RIVM, Bilthoven, 2001.
Pacyna, E. G. and Pacyna, J. M.: Global emission of mercury from anthropogenic sources in 1995, Water Air Soil Pollut., 137, 149–165, 2002.
Pacyna, J. M., Pacyna, E. G., Steenhuisen, F., and Wilson, S.: Mapping 1995 global anthropogenic emissions of mercury, Atmos. Environ., 37, 109–117, 2003.
Pacyna, E. G., Pacyna, J. M., Steenhuisen, F., and Wilson, S.: Global anthropogenic mercury emission inventory for 2000, Atmos. Environ., 40, 4048–4063, 2006.
Pacyna, E. G., Pacyna, J. M., Sundseth, K., Munthe, J., Kindbom, K., Wilson, S., Steenhuisen, F., and Maxson, P.: Global emission of mercury to the atmosphere from anthropogenic sources in 2005 and projections to 2020, Atmos. Environ., 44, 2487–2499, 2010.

ACPD
12, 11079–11103, 2012

Pirrone, N., Keeler, G. J., and Nriagu, O.: Regional differences in worldwide emissions of mercury to the atmosphere, Atmos. Environ., 30, 2981–2987, 1996.
Pirrone, N., Allegrini, I., Keeler, G. J., Nriagu, J. O., Rossmann, R., and Robbins, J. A.: Historical atmospheric mercury emissions and depositions in North America compared to mercury accumulations in sedimentary records, Atmos. Environ., 32, 929–940, 1998.
Pirrone, N., Cinnirella, S., Feng, X., Finkelman, R. B., Friedli, H. R., Leaner, J., Mason, R., Mukherjee, A. B., Stracher, G. B., Streets, D. G., and Telmer, K.: Global mercury emissions to the atmosphere from anthropogenic and natural sources, Atmos. Chem. Phys., 10, 5951–5964, doi:10.5194/acp-10-5951-2010, 2010.
Scheel, H. E., Brunke, E.-G., and Seiler, W.: Trace gas measurements at the monitoring station Cape Point, South Africa, between 1978 and 1988, J. Atmos. Chem., 11, 197–210, 1990.
Scheuhammer, A. M., Meyer, M. W., Sandheinrich, M. B., and Murray, M. W.: Effects of environmental methylmercury on the health of wild bird, mammals, and fish, Ambio, 36, 12–18, 2007.
Selin, N. E., Jacob, D. J., Park, R. J., Yantosca, R. M., Strode, S., Jaeglé, L., and Jaffe, D.: Chemical cycling and deposition of atmospheric mercury: global constraints from observations, J. Geophys. Res., 112, D02308, doi:10.1029/2006JD007450, 2007.
Selin, N. E., Jacob, D. J., Yantosca, R. M., Strode, S., Jaeglé, L., and Sunderland, E. M.: Global 3-D land-ocean-atmosphere model for mercury: present-day versus preindustrial cycles and anthropogenic enrichment factors for deposition, Global Biogeochem. Cy., 22, GB2011, doi:10.1029/2007GB003040, 2008.
Singh, H. B., Anderson, B. E., Brune, W. H., Cai, C., Cohen, R. C., Crawford, J. H., Cubison, M. J., Czech, E. P., Emmons, L., Fuelberg, H. E., Huey, G., Jacob, D. J., Jimenez, J. L., Kaduwela, A., Kondo, Y., Mao, J., Olson, J. R., Sachse, G. W., Vay, S. A., Weinheimer, A., Wennberg, P. O., Wisthaler, A., and the ARCTAS Science Team: Pollution influences on atmospheric composition and chemistry at high northern latitudes: boreal and California forest fire emissions, Atmos. Environ., 44, 4553–4564, 2010.
Slemr, F., Baumbach, G., Blank, P., Friedrich, R., Habram, M., Kalthoff, N., Klemp, D., Kühlwein, J., Mannschreck, K., Möllmann-Coers, M., Nester, K., Panitz, H.-J., Rabl, P., Slemr, J., Vogt, U., and Wickert, B.: Evaluation of modeled spatially and temporarily highly resolved emission inventories of photo smog precursors for the city of Augsburg: the experiment EVA and its major results, J. Atmos. Chem., 42, 207–233, 2002.

ACPD
12, 11079–11103, 2012

Slemr, F., Ebinghaus, R., Simmonds, P. G., and Jennings, S. G., European emissions of mercury derived from long-term observations at Mace Head, on the Western Irish Coast, Atmos. Environ., 40, 6966–6974, 2006.
Streets, D. G., Hao, J., Wu, Y., Jiang, J., Chan, M., Tian, H., and Feng, X.: Anthropogenic mercury emissions in China, Atmos. Environ., 39, 7789–7806, 2005.
Streets, D. G., Zhang, Q., and Wu, Y.: Projections of global mercury emissions in 2050, Environ. Sci. Technol., 43, 2983–2988, 2009.
Strode, S. A., Jaeglé, L., Selin, N. E., Jacob, D. J., Park, R. J., Yantoska, R. M., Mason, R. P., and Slemr, F.: Air-sea exchange in the global mercury cycle, Global Biogeochem. Cy., 21, GB1017, doi:10.1029/2006GB002766, 2007.
van der Werf, G. R., Randerson, J. T., Giglio, L., Collatz, G. J., Kasibhatla, P. S., and Arellano Jr., A. F.: Interannual variability in global biomass burning emissions from 1997 to 2004, Atmos. Chem. Phys., 6, 3423–3441, doi:10.5194/acp-6-3423-2006, 2006.
WMO: Technical Report No. 161, Geneva, Switzerland, 2005.
Wilson, S. J., Steenhuisen, F., Pacyna, J. M., and Pacyna E. G.: Mapping the spatial distribution of global anthropogenic mercury atmospheric emission inventories, Atmos. Environ., 40, 4621–4632, 2006.

ACPD
12, 11079–11103, 2012

Table 1. Statistics of 67 identified PEs and their slopes of correlation for Hg/CO, Hg/CO_2, Hg/CH_4, CO/CO_2, CH_4/CO_2, and CH_4/CO.

Correlation	Events with available data	Significant correlations > 95 %	Range	Slope Average	Median
GEM/CO ($pg\,m^{-3}\,ppb^{-1}$)	67	47	0.20–11.5	2.40 ± 2.65	1.41
GEM/CO_2 ($pg\,m^{-3}\,ppm^{-1}$)	63	44	12.3–436	62.7 ± 80.2	34.1
GEM/CH_4 ($pg\,m^{-3}\,ppb^{-1}$)	67	46	0.365–24.8	3.61 ± 4.66	2.13
CO/CO_2 ($ppb\,ppm^{-1}$)	63	52	3.98–169	35.6 ± 25.4	30.1
CH_4/CO_2 ($ppb\,ppm^{-1}$)	63	48	1.05–77.3	20.2 ± 15.5	15.7
CH_4/CO ($ppb\,ppb^{-1}$)	67	42	0.092–6.62	0.876 ± 1.106	0.508

ACPD
12, 11079–11103, 2012

Table 2. Average and median slopes of GEM/CO, GEM/CO_2, GEM/CH_4, CO/CO_2, CH_4/CO_2, and CH_4/CO for different trajectory types. Average, standard deviation and number of slopes are given in the upper line, medians in the lower line.

Trajectory type	1	2	3	4
GEM/CO ($pg\,m^{-3}\,ppb^{-1}$)	1.30 ± 1.15 (12) 0.90	2.69 ± 2.52 (5) 1.23	3.51 ± 4.48 (5) 1.63	2.65 ± 2.74 (25) 1.51
GEM/CO_2 ($pg\,m^{-3}\,ppm^{-1}$)	26.8 ± 9.3 (9) 30.5	49.9 ± 45.7 (5) 25.3	37.8 ± 15.8 (4) 32.4	81.5 ± 98.5 (26) 50.2
GEM/CH_4 ($pg\,m^{-3}\,ppb^{-1}$)	2.53 ± 3.21 (13) 2.10	3.09 ± 2.22 (6) 2.89	1.73 ± 0.51 (3) 1.68	4.57 ± 5.81 (24) 2.63
CO/CO_2 ($ppb\,ppm^{-1}$)	36.4 ± 21.8 (12) 28.6	31.6 ± 13.8 (8) 31.5	26.1 ± 15.1 (4) 20.9	37.7 ± 30.5 (28) 30.9
CH_4/CO_2 ($ppb\,ppm^{-1}$)	15.8 ± 9.4 (12) 14.5	17.3 ± 15.9 (7) 13.4	19.4 ± 7.5 (3) 16.9	23.2 ± 18.0 (26) 17.2
CH_4/CO ($ppb\,ppb^{-1}$)	0.517 ± 0.269 (11) 0.421	0.528 ± 0.304 (7) 0.571	1.029 ± 0.651 (3) 0.859	1.159 ± 1.484 (21) 0.444

ACPD
12, 11079–11103, 2012

Table 3. Comparison of CO/CO_2, CH_4/CO_2, and CH_4/CO emission ratios from observations and from EDGAR inventory and GEM emissions calculated from GEM/CO, GEM/CO_2, and GEM/CH_4 emission ratios.

		South Africa	Southern Africa [a]
CO_2 emission [b] ($Tg\,yr^{-1}$)		476.0	572.7
CO emission [b] ($Tg\,yr^{-1}$)		6.968	9.898
CH_4 emission [b] ($Tg\,yr^{-1}$)		3.174	4.515
CO/CO_2 ER ($ppb\,ppm^{-1}$)	calculated	23.0	27.2
	observed	35.6 ± 25.4 (n = 52), median 30.1	
CH_4/CO_2 ER ($ppb\,ppm^{-1}$)	calculated	18.3	21.7
	observed	20.2 ± 15.5 (n = 48), median 15.7	
CH_4/CO ER ($ppb\,ppb^{-1}$)	calculated	0.797	0.798
	observed	0.876 ± 1.106 (n = 42), median 0.508	
GEM emissions ($t\,yr^{-1}$)	from GEM/CO ER	13.1	18.3
	from GEM/CO_2ER	15.2	18.6
	from GEM/CH_4ER	16.1	22.9

[a] South Africa and neighbors (Lesotho, Swaziland, Namibia, Botswana, Zimbabwe, and Mozambique).
[b] Including emissions from biomass burning, annual average of 2007 and 2008.

ACPD
12, 11079–11103, 2012

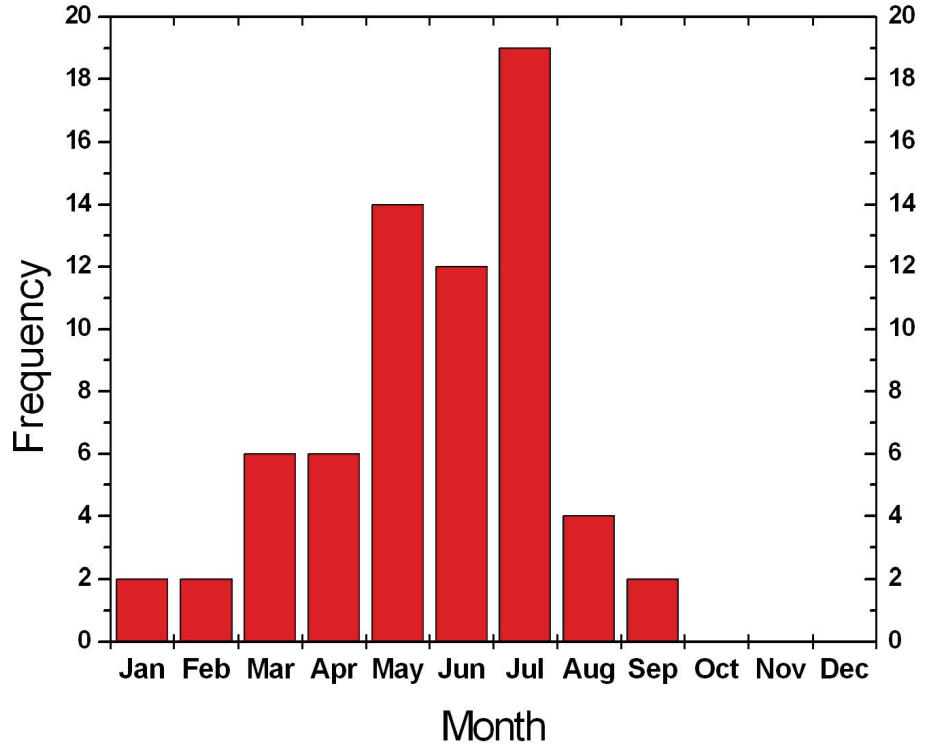

Fig. 1. Seasonal frequency of PE occurrence.

ACPD
12, 11079–11103, 2012

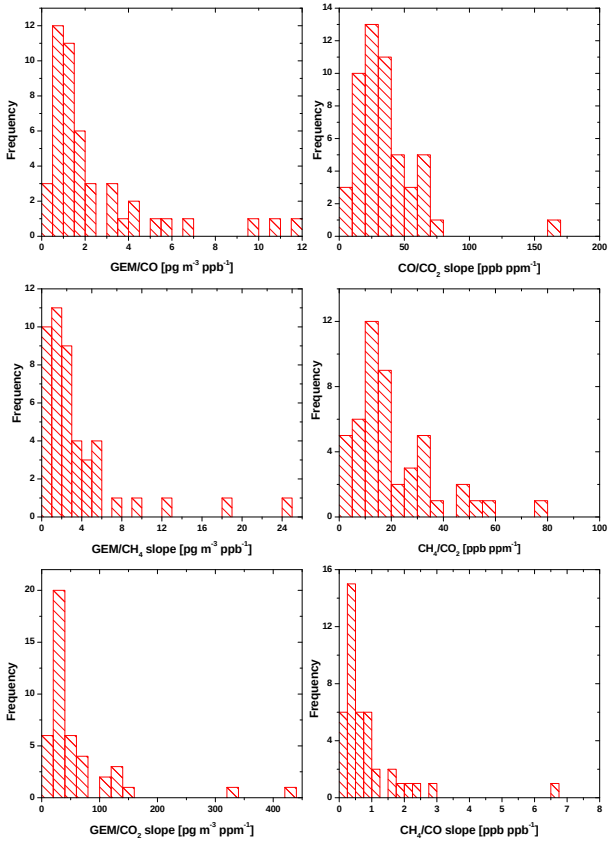

Fig. 2. Frequency distribution of GEM/CO, GEM/CO_2, GEM/CH_4, CO/CO_2, CH_4/CO_2, and CH_4/CO slopes.

ACPD
12, 11079–11103, 2012

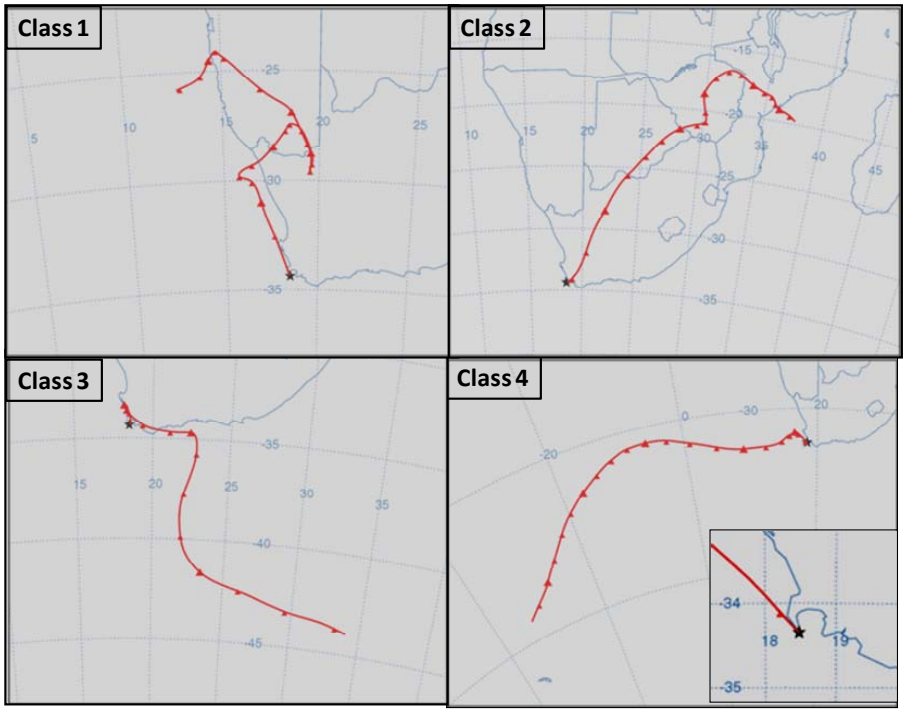

Fig. 3. Examples of the most frequent types of backward trajectories for pollution events observed at Cape Point: class 1: North-West Cape (with a subgroup 1 (CT): Cape Town, trajectory from 27 May, 2008, 11:00 UTC); class 2: Gauteng, Mpumalanga, Botswana, Zimbabwe (trajectory from 18 June, 2008, 15:00 UTC); class 3: East Cape Province (trajectory from 2 June, 2008, 14:00 UTC); class 4: marine with short section over the continent, i.e. local pollution (trajectory from 26 July, 2008, 13:00 UTC).

ACPD
12, 11079–11103, 2012